

# Local Heat-Transfer Coefficients of Simulated Smooth Glaze Ice Formations on a Cylinder

Martin Pais\* and S.N. Singh†  
University of Kentucky, Lexington, Kentucky

Experimental convective local heat-transfer coefficients were obtained for a simulated, selected set of smooth 2-, 5-, and 15-min glaze ice profiles formed on the surface of a 50.8-mm cylinder in cross flow. A steady-state heat-flux method was employed. The velocity and turbulence intensity distributions and the local heat-transfer rates are measured as a function of Reynolds number. The Nusselt numbers obtained in the Reynolds number range 100,000–150,000 were compared with those obtained in previous experiments. The results show very good quantitative and qualitative agreement. The local heat-transfer rate increases with increasing Reynolds number and appears to decrease as the ice grows.

## Nomenclature

|        |                                  |
|--------|----------------------------------|
| $A$    | = surface area                   |
| $B$    | = blockage ratio                 |
| $D$    | = diameter of cylinder           |
| $h$    | = heat-transfer coefficient      |
| $I$    | = current, A                     |
| $k$    | = thermal conductivity           |
| $Nu$   | = Nusselt number, $hD/k$         |
| $q$    | = heat flux                      |
| $Re$   | = Reynolds number, $\rho UD/\mu$ |
| $T$    | = temperature                    |
| $U$    | = velocity                       |
| $V$    | = voltage, V                     |
| $w$    | = liquid water content           |
| $\rho$ | = density                        |
| $\mu$  | = viscosity                      |
| $\tau$ | = time                           |

## Subscripts

|          |           |
|----------|-----------|
| $w$      | = wall    |
| $\infty$ | = ambient |

## Introduction

IN recent years, the problem of ice formation on aircraft has received considerable attention because of its influence on military aircraft capabilities. Two symposia have been held exclusively on the ice accretion processes, and papers presented in these meetings, along with discussion, have been published in two AGARD reports.<sup>1,2</sup> In addition, a special session on icing phenomena was arranged by the American Institute of Aeronautics and Astronautics at its Aerospace Sciences Meeting in January 1981.<sup>3</sup>

Ice formation on aircraft is one of the greatest dangers to air safety. Two principal types of ice have been observed to form on parts of aircraft, namely, glaze and rime. The formation of ice depends on six parameters:<sup>4</sup> the ambient temperature ( $T_\infty$ ), liquid water content ( $w$ ), droplet diameter ( $d$ ), aircraft velocity ( $U_\infty$ ), airfoil geometry ( $y=f(x)$ ), and icing time ( $\tau$ ).

The formation of ice on aircraft structures can increase their drag and weight. In addition, ice may lead to control problems and, if it sloughs off, damage structures downstream. Ingested ice can also damage jet engines. The above situation can cause serious problems for successful missions of cruise missiles flying over the North Atlantic and North Sea. In Europe in winter, it is possible to have the proper weather conditions for ice formation up to 30% of the time.

The thermodynamic conditions for either rime or glaze ice to form on structures are well understood. Several empirical theories have been developed that can predict the amount of ice formed. These theories rely, however, on questionable application of heat-transfer results that were obtained for other flow conditions.

Plaster casts of ice growth on a 50.8-mm cylinder were obtained at certain time intervals from experiments conducted in the icing research tunnel at NASA Lewis. The profiles obtained were smoothed, and coordinates of the same were provided to the authors by Shaw.<sup>8</sup> The icing conditions were as follows: liquid water content,  $w=2.1$  g/m<sup>3</sup>, average droplet size  $d=20$   $\mu$ m,  $T_\infty=-7.8^\circ$ C,  $U_\infty=130$  mph. The shape of the growth of glaze ice on a cylinder (smoothed profile) is shown in Fig. 1. The horn-shaped structure is characteristic for glaze ice, and the major protrusions occur in the regions of maximum heat transfer. These protrusions become relatively large compared to the boundary-layer thickness and affect the flow and heat-transfer characteristics of the surface. The local heat-transfer rates are needed to predict the ice formation and growth rates.

Laboratory-scale experiments were conducted in the subsonic wind-tunnel facility at the University of Kentucky. The structure was instrumented to measure velocity and turbulence intensity distributions and the local heat-transfer rate. The full-scale models were locally heated using thermofoil heaters, and the temperature was monitored by a grid of thermocouples. When isothermal conditions were attained on the surface, the heat flux was equal to the electric power input. Measurements from three smooth glaze ice models (2, 5, and 15 min) on a cylinder were obtained and compared with data available from VanFossen<sup>10</sup> and Arimilli.<sup>11</sup>

## Apparatus

The experiment was conducted in the subsonic wind-tunnel facility in the Department of Mechanical Engineering at the University of Kentucky. The induced-flow wind tunnel is equipped with a 50-kW axial fan and has, at the upstream end of the plenum chamber, a 4.8-mm honeycomb, 102-mm in depth, for straightening the flow. The 508 mm  $\times$  711

Received June 17, 1985; revision received July 7, 1986.  
Copyright © American Institute of Aeronautics and Astronautics, Inc., 1987. All rights reserved.

\*Graduate Research Assistant, Department of Mechanical Engineering. AIAA Student Member.

†Professor, Department of Mechanical Engineering.

mm × 1220 mm test section has three sides made of plexiglass for future use in flow visualization. Ports are provided in the sides for taking velocity measurements using a hot-film probe over a three-dimensional grid. Velocities up to 160 mph can normally be realized in this section. The glaze ice model is attached to a cylinder held vertically and clamped firmly at its ends. The model is aligned with the direction of the flow using two static pressure ports equally spaced from a reference stagnation point on the cylindrical body.

The surface of the models is heated using many independent Minco thermofoil heaters, 5.9 mm × 175 mm × 0.3 mm, glued on, with the long sides touching, to the white pine body of the model using Omega 101 epoxy (see Fig. 2). This wooden model is then attached to a 50.8-mm, thin-walled (1.7-mm) brass cylinder, closed at both ends to minimize heat losses due to free convection from within. Each heater has an individual power supply. The voltage across each heater is measured using an HP 3455A digital voltmeter. The current through each heater is measured by a FLUKE 8600A digital multimeter. A bank of quick disconnects makes it possible to connect the one ammeter in series with any heater circuit, one at a time. Each heater has a 0.02-mm Inconel element, which has a negligible temperature coefficient of resistance in the temperature range of interest.

The temperature of each individual heater is monitored using three OMEGA 1-mm copper-constantan thermocouples placed equidistantly along the length. This not only provides a temperature distribution on the surface but also acts as a backup feature in case any one thermocouple malfunctions. This latter precaution is necessary since the temperature of the entire surface has to be maintained in an isothermal state within experimental limits. The thermocouple junctions are affixed to the top of the heater surface using a highly conductive Omega 101 epoxy as a heat sink. Thermocouples are also placed at the junction of the ice profile with the cylinder in order to measure the base cylinder temperature from which an estimate of the conductive heat losses through the wooden model can be calculated. The whole assembly is finally covered with adhesive-backed, thin (0.07-mm) aluminum foil to give a smooth, continuous surface. Because the foil is thin, it is assumed not to affect the heat transfer into the airstream. Also, the low emissivity of aluminum reduces heat losses due to radiation. Calibrated Omega electronic ice points are used in conjunction with the thermocouples, and these voltages are read and recorded using an HP 3467A logging multimeter. Electrical access to any heater or thermocouple is facilitated through a bank of scanners. The freestream temperature  $T_\infty$  is measured by a separate thermocouple mounted on the unheated section of the cylinder inside the tunnel.

The velocity is measured using a TSI 1210-20 single hot-film sensor controlled by a TSI 1050 series constant

temperature anemometer. A DISA 55D35 RMS voltmeter provides the turbulence intensity. The linear response of the anemometer was checked using a standard nozzle with a 3.41:1 contraction ratio, a stilling chamber, and a flow straightener. The nozzle upstream pressure was measured by a Miriam Micromanometer to within ±0.025 mm of water. The setup was designed by Abdelghany<sup>7</sup> to supply a low-turbulence airjet, free of swirl.

Experimental Procedure

Newton's Law of Cooling,

$$q = hA(T_w - T_\infty) \quad (\text{watts}) \quad (1)$$

defines the convective heat flux between a fluid at temperature  $T_\infty$  in contact with a surface at temperature  $T_w$ . The proportionality constant  $h$  (W/m<sup>2</sup> K) is referred to as the heat-transfer coefficient. It depends on the conditions within the boundary layer, which are a function of the surface

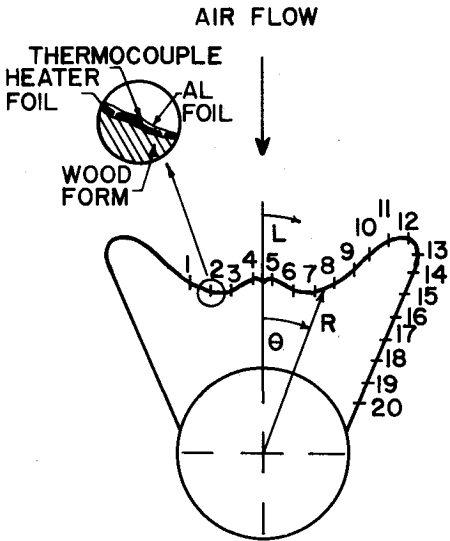


Fig. 2 Heater and thermocouple layout on ice model.

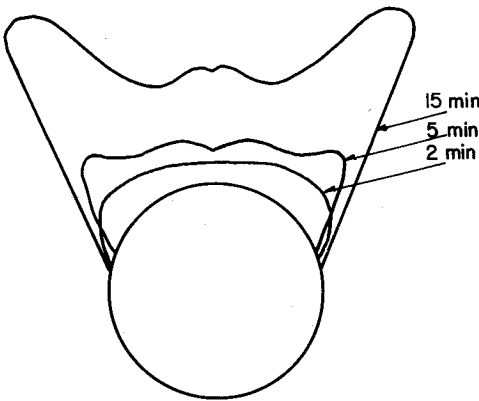


Fig. 1 2-, 5-, and 15-min glaze ice profiles.

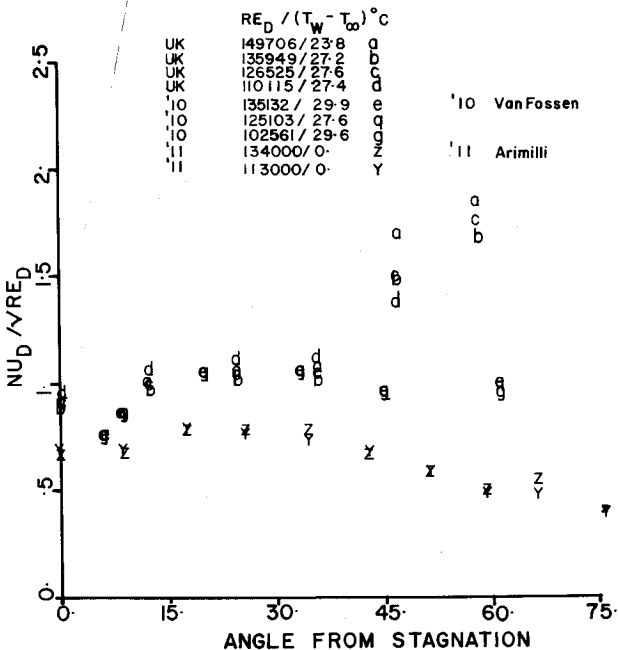


Fig. 3 Local heat-transfer coefficient on 2-min model.

geometry, the nature of the fluid motion, and fluid thermodynamic and transport properties.<sup>5,6</sup> In applying this law to our problem of glaze ice accretion, a case in which we have a mass of water being transferred from the fluid to the body surface by freezing due to convective heat loss, we can assume an isothermal surface at a temperature equal to that of the freezing point of water. Lack of experimental facilities limit an exact simulation. If, however, we consider the glaze ice at any instant in time and assume no further ice accretion, then the geometry is fixed. The heat-transfer coefficient can then be approximated experimentally as long as one can reproduce the geometry and flow conditions (Reynolds number) and provide an isothermal surface to ensure a similar thermal boundary layer. If the above conditions are satisfied, the heat-transfer coefficient can be evaluated from knowledge of the local heat flux and respective temperatures required by Newton's law of cooling.

In these experiments, the problem of maintaining a uniform temperature on the surface is solved by using narrow strips of Minco thermofoil heaters as part of the surface of the glaze ice (see Fig. 2). The temperature of the surface is measured using thermocouples. Hence, if the model is made of insulating material, (white pine was used in these experiments), all the heat must be dissipated directly into the fluid medium. The electrical energy input is converted into thermal energy in the resistance of the heaters, which essentially is our required heat flux.

$$q = V \times I \quad (\text{watts}) \quad (2)$$

A selected set of 2-, 5-, and 15-min smooth glaze ice profiles were prepared as described in the preceding section. The wind tunnel was allowed to run for 5–10 min in order to attain steady flow and temperature conditions. The velocity was set to obtain a predetermined Reynolds number. The power to the individually controlled heaters was switched on, and the thermocouple temperatures were continuously monitored until a constant temperature was attained over the surface. Once steady-state conditions were reached, the voltage across, the current through, and the thermocouple voltages on each heater were noted. Finally, the freestream temperature and velocity were recorded.

A TSI 1210-20 single hot-film sensor was used to measure the velocity and intensity of turbulence in the wind tunnel at the University of Kentucky. The probe was connected to a TSI 1050 series constant temperature anemometer system, from which the linearized signal is measured by a HP 3455A digital voltmeter and a DISA 55D35 RMS voltmeter.

The calibration of the hot wire indicates a correlation coefficient of 0.998 or better. Calibrations were performed before each experiment to take care of changes in temperature and weather. Using the hot-film probe, a profile of the velocities within the test section was performed over a 16 × 27 grid. The velocity was observed to be uniform over the test section. The maximum intensity of turbulence in the central region was of the order of 0.5%. As stated earlier, the models are equipped with three sets of thermocouples: top, middle, and bottom rows, respectively. In performing the experiment, it is necessary to select which one of the rows will determine the constant surface temperature condition, (generally, the choice would be the middle row from symmetry considerations). This is necessary because once the power to a heater is set with respect to one of its thermocouples, the temperature indicated by the remaining two is automatically fixed. No other control is available to change their output without changing the initial setting. Hence, at steady state, we will have a band around the model in which the temperature is constant. The other regions may have slight temperature variations. The authors used this isothermal band for the calculation of the necessary parameters of this study. Note that this assumption is valid because the temperature coefficient of resistance of the ther-

mofoil heater is negligible in the temperature range of interest.

## Results

The experimental setup at the University of Kentucky was first tested to obtain reliable measured results. To do this, an initial experiment was performed to measure the local heat-transfer coefficient on a 2-in. cylinder using the steady-state heat-flux method. The data obtained agree very well with published results.<sup>5,9</sup>

### Two-Minute Glaze Ice on a Circular Cylinder

This protrusion covers 116 deg of angular surface, or a total nondimensional length ( $L/D$ ) of 1.35. The blockage ratio for the model is equal to 0.078. The maximum variation in temperature is 1.0% over the entire central band at a surface temperature of 48°C. The mean of the local heat-transfer coefficient of symmetric points about the forward stagnation (location 0 deg) was taken. This procedure showed a  $\pm 47$  variation in the  $Nu_D$  number and a  $\pm 0.12$  variation in the  $Nu_D/\sqrt{Re_D}$  at any location. Radiation losses were minimal at 0.3%, and conduction losses were measured and assessed not to be greater than 5%, which occurred at the junction of ice with the cylinder.

Figure 3 is a plot of  $Nu_D/\sqrt{Re_D}$  vs angle, which compares the results with those of VanFossen<sup>10</sup> and Arimilli.<sup>11</sup> This

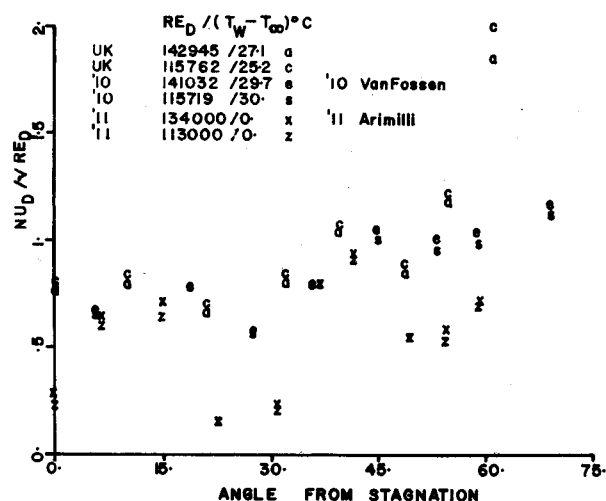


Fig. 4 Local heat-transfer coefficient on 5-min model.

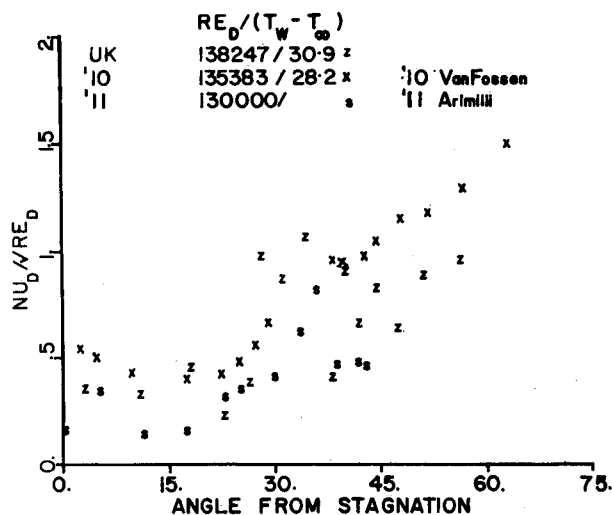


Fig. 5 Local heat-transfer coefficient on 15-min model.

shows that the authors' data compare extremely well with those of VanFossen<sup>10</sup> over most of the region. We also find much higher values at the junction of the ice with the cylinder in the downstream end. This may be due to the higher curvature in this section of the model. Arimilli<sup>11</sup> shows the same qualitative trend but is lower by around 13% on the average, with the authors' data as the base.

#### Five-Minute Glaze Ice on a Circular Cylinder

This ice shape covers 122 deg of angular surface or a total nondimensional length ( $L/D$ ) of 1.89. The blockage ratio for this model is equal to 0.088. The maximum temperature variation is around 1.0% over the entire central band at a surface temperature of 52°C. The mean of the local heat-transfer coefficient of symmetric points about the forward stagnation was taken. This procedure shows on the average a  $\pm 14$  variation in the  $Nu_D$  number and a  $\pm 0.04$  variation in the  $Nu_D/\sqrt{Re_D}$  at any point. Radiation losses were less than 0.3%, and conduction losses were measured and assessed to

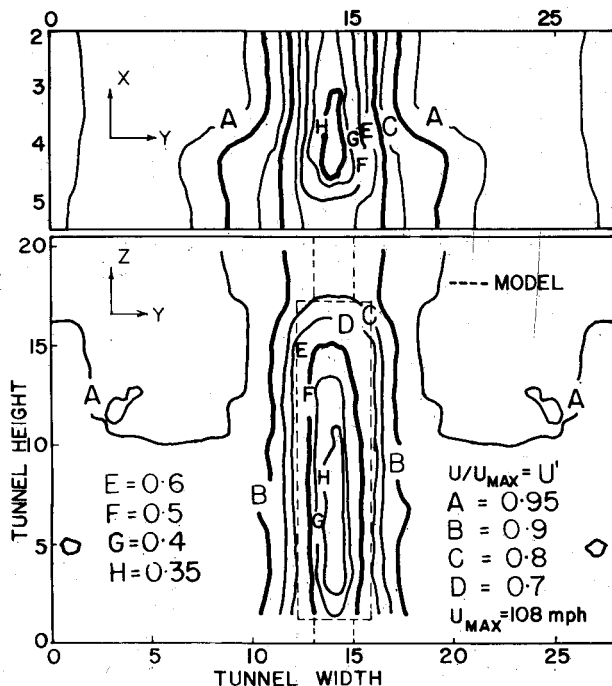


Fig. 6 Velocity contours upstream of 15-min model.

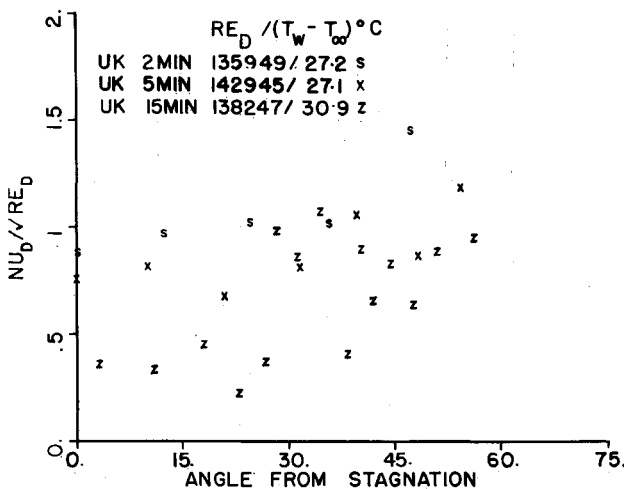


Fig. 7 Comparison of heat-transfer coefficient with ice growth.

be not greater than 3%, which occurred at the junction of the ice with the cylinder.

The data of VanFossen,<sup>10</sup> Arimilli,<sup>11</sup> and the authors are compared in Fig. 4. This shows very good agreement between VanFossen<sup>10</sup> and the present data. The authors' data show much higher values at the junction of the ice with the cylinder in the downstream end. This again is because of the higher curvature in this section of the model. Arimilli<sup>11</sup> shows the same qualitative trend but is lower by around 75% maximum, with the present data as the base.

#### Fifteen-Minute Glaze Ice on a Circular Cylinder

This model covers 125 deg of angular surface or a total nondimensional length ( $L/D$ ) of 4.2. The blockage ratio for this model is equal to 0.132. The maximum temperature variation is around 1.0% over the entire band at a surface temperature of 55°C. The mean of the local heat-transfer coefficients at symmetric points about the forward stagnation was taken. This procedure shows on the average a  $\pm 44$  variation in the  $Nu_D$  number and a  $\pm 0.12$  variation in the  $Nu_D/\sqrt{Re_D}$  at any location. Radiation losses were less than 1.2% and conduction losses were measured and assessed not to be greater than 4%, which occurred at the junction of the ice with the cylinder.

Figure 5 shows a comparison of the data with published results from VanFossen<sup>10</sup> and Arimilli.<sup>11</sup> The authors' data compare in trend with those of VanFossen<sup>10</sup> over most of the region, showing values lower than those of VanFossen<sup>10</sup> at times by up to a relative error of 27%, based on the authors' data. Past the horn of the protrusion and downstream, the heat-transfer coefficient is observed to follow a wave-like function, which starts at an angle of 35 deg from the forward stagnation point (0 deg). A numerical flow study on the same profile performed by Calarese<sup>12</sup> lends credence to this behavior. The flow, going around the horn, encounters downstream regions of separation and reattachment, which would cause sudden changes in the thermal boundary layer and, hence, the undulating form of the local heat-transfer coefficient. Arimilli<sup>11</sup> follows the trend up to the stagnation point at the horn but falls off rapidly in magnitude farther downstream.

A study of the velocity field, ahead of the 15-min model, in a three-dimensional grid between 76 and 140 mm upstream from the center of the cylinder is shown in Fig. 6. This is a contour plot in the YZ and YX planes of the non-dimensional velocity, based on the maximum velocity in the X direction, i.e., the direction of flow. The velocity profile in the region of interest is noted to be uniform and symmetric about the longitudinal axis of the model. A large stagnation zone exists upstream of the profile, where velocities drop to less than 40% of the freestream up to 2 diameters away. In the case of the 15-min profile, the stagnation zone extends up to approximately 305 mm, (6 diameters), upstream from the center of the cylinder. It is also observed that secondary flows exist in both the XY and XZ planes. These are not exactly symmetric and may be the cause of asymmetries in the boundary-layer flow, leading to the variation in the heat-transfer coefficients measured at locations symmetric about the forward stagnation.

The comparison of the local heat-transfer rates for the three profiles shown in Fig. 1 is provided in Fig. 7. It is observed that as the ice grows on the cylinder, the heat-transfer coefficient at any region decreases. This can be explained by noting that as the ice grows, it takes up a two-dimensional concave profile in the forward stagnation zone. This tends to enlarge the upstream stagnation zone, which may extend many diameters ahead. This results in a slower-moving and thicker thermal boundary layer, which results in the heat-transfer coefficient being lowered.

Calculations were done to correlate some characteristic dimension of the profile, which includes ice growth, with the Nusselt number. When the Nusselt number is based on the

maximum width of the profile subtended by the flow, the data from the different ice profiles tend to coalesce. A better correlation also exists between  $Nu_D/\sqrt{Re_D}$  and angle than between  $Nu_D/\sqrt{Re_D}$  and  $L/D$ .

### Conclusions

The technique used by the authors to measure the heat-transfer coefficient gave good, reproducible results. The smooth ice shape models were prepared meticulously, with precautions taken to conform to the initial profile as closely as possible. Heat-transfer results agree well with those of VanFossen.<sup>10</sup> Arimilli's<sup>11</sup> data show similar trends but are lower in magnitude. It must be stated here that both the VanFossen<sup>10</sup> and the authors' models were almost identical in size and shape. Arimilli,<sup>11</sup> used a transient method to measure the heat-transfer coefficient, and his models were geometrically similar but mounted on a cylinder 63.5 mm in diameter. A better correlation exists between Nusselt number and angle from stagnation than between the Nusselt number and  $L/D$ .

The heat-transfer coefficient decreases with growth of the ice. When the Nusselt number is based on the maximum width of the profile subtended to the flow, which includes the ice growth, the data from the different ice profiles tend to coalesce.

### Recommendations

More experiments must be performed to try to find some characteristics that can better depict any general ice growth. Further work is currently being performed on rough glaze ice shapes on cylinders and on a NACA 0012 airfoil.

### Acknowledgments

The authors would like to thank the Air Force Systems Command and the Computational Aerodynamics Group at

the Flight Dynamics Laboratory, Wright-Patterson Air Force Base, Dayton, Ohio, for providing them the opportunity to do research on ice formation characteristics on cylinders and airfoils. They would like to thank Dr. Wilbur Hankey and Dr. Wladimiro Calarese for their several suggestions and helpful discussion. Help rendered by Dr. R.C. Birkebak at the initial stage is also acknowledged.

### References

- <sup>1</sup>"Aircraft Icing," AGARD-AR-127, 1977.
- <sup>2</sup>"Icing Testing for Aircraft Engines," AGARD-CP-236, 1978.
- <sup>3</sup>AIAA 19th Aerospace Sciences Meeting, St. Louis, MO, Jan. 12-15, 1981, Session 72, Aircraft Icing.
- <sup>4</sup>Hankey, W.L. and Kirchner, R., "Ice Accretion of Wing Leading Edges," AFFOL-TM-79-85-FXM, June, 1979.
- <sup>5</sup>Incropera, F.P. and DeWitt, D.P., *Fundamentals of Heat Transfer*, Wiley, New York, 1981, pp. 340-350.
- <sup>6</sup>Kays, W.M. and Crawford M.E., *Convective Heat and Mass Transfer*, 2nd ed., McGraw-Hill, New York, 1980, pp. 139-158.
- <sup>7</sup>Abdelghany, M.M., "Experimental Study of Axial Flow in a Finite Array of Rods and the Application of Finite Element Techniques to Flow in Ducts and Rod Bundles," Ph.D. Thesis, University of Kentucky, Lexington, pp. 27-29.
- <sup>8</sup>Shaw, J., NASA Lewis Research Center, Cleveland, OH.
- <sup>9</sup>Schlichting, H., *Boundary Layer Theory*, 7th ed., McGraw-Hill, New York, 1979, pp. 456-457.
- <sup>10</sup>VanFossen, G.J., Simoneau, R.J., Olsen, W.A. Jr., and Shaw, R., "Heat Transfer Distributions Around Nominal Ice Accretion Shapes Formed on a Cylinder in the NASA Lewis Icing Research Tunnel," AIAA Paper 84-0017, Jan. 1984.
- <sup>11</sup>Arimilli, R.V., Keshock, E.G., and Smith, M.E., "Measurements of Local Convective Heat Transfer Coefficients on Ice Accretion Shapes," AIAA Paper 84-0018, Jan. 1984.
- <sup>12</sup>Calarese, W. and Barth, T.J., "Numerical Simulation of Heat Transfer Rates on an Ice Accretion Model," AFWAL-TM-85-191-FIMM, Dec. 1984.